Title

Three-dimensional analysis of subchondral cysts in hip osteoarthritis: An ex vivo HR-pQCT study

Authors

Chiba, Ko
Burghardt, Andrew J
Osaki, Makoto
et al.

Publication Date

2014-09-01

DOI

10.1016/j.bone.2014.06.001

Peer reviewed

Published in final edited form as:
Bone. 2014 September ; 66: 140–145. doi:10.1016/j.bone.2014.06.001.

Three-dimensional Analysis of Subchondral Cysts in Hip Osteoarthritis: an *ex vivo* HR-pQCT study

Ko Chiba[1,2], **Andrew J. Burghardt**[1], **Makoto Osaki**[2], and **Sharmila Majumdar**[1]

[1]Musculoskeletal Quantitative Imaging Research Group, Department of Radiology and Biomedical Imaging, University of California, San Francisco; San Francisco, CA USA

[2]Department of Orthopedic Surgery, Nagasaki University School of Medicine; Nagasaki, Japan

Abstract

Introduction—Subchondral cysts are deeply related to the pathogenesis of osteoarthritis (OA), but the factors contributing to cyst formation are not well known. A three-dimensional analysis of subchondral cysts at the micro-structural level was conducted using high-resolution peripheral quantitative CT (HR-pQCT), and their relationships with cartilage attrition and subchondral bone microstructure were investigated.

Methods—Femoral heads extracted from ten female patients with hip OA were scanned using HR-pQCT at a voxel size of 41 μm. The volume fractions, numbers, and sizes of the cysts were measured in the subchondral bone region under the area of cartilage loss. Furthermore, the areas of cartilage loss, as well as the microstructure of the subchondral bones, were also measured, and their correlations with the cysts were analyzed.

Results—The volume fractions of cysts within subchondral bone regions varied from 2% to 33%, the numbers of cysts varied from 6 to 87, and the sizes varied from 1 mm^3 to 657 mm^3. There was a positive correlation between the number of cysts and bone volume ($r>0.8$, $p<0.01$).

Conclusion—The degree of cyst formation showed a wide distribution in number and volume, and there was a close relationship between multiple cyst formation and bone sclerosis, which might be caused by reactive bone formation that occurred around each cyst.

Keywords

Osteoarthritis; Subchondral Cyst; HR-pQCT; Subchondral Bone; Microstructure

Corresponding author: Ko Chiba Department of Orthopedic Surgery, Nagasaki University School of Medicine 1-7-1, Sakamoto, Nagasaki 852-8501, Japan kohchiba@estate.ocn.ne.jp.

Competing Interests None.

Author Contributions KC: design, collection and analysis of data, and drafting of the article
AB and SM: design, collection and analysis of data, and revision of the article
MO: collection of data

Introduction

Osteoarthritis (OA) is a degenerative joint disease characterized by cartilage attrition and joint pain. In recent years, there has been interest in the role of subchondral bone in the pathogenesis of OA. In the subchondral bone of OA, enhanced bone turnover, activation of cells such as osteoblasts, and production of chemical substances such as inflammatory cytokines and proteinases have been confirmed. Although it remains controversial, it has been considered that these changes are associated with induction of cartilage attrition. (1-3)

Subchondral bone of OA shows various changes in trabecular structure, such as bone sclerosis; pathological thickening of trabecular bones, and subchondral cysts; cavity formation by trabecular bone resorption**.** Subchondral cysts are thought to be formed by bone resorption due to bone contusion by excessive mechanical stress or synovial fluid intrusion into bone marrow spaces. (4-6) Histologically, activated osteoclasts and osteoblasts have been identified around subchondral cysts. (7,8) A study using synchrotron radiation micro CT, which can visualize the degree of mineralization of trabecular bone accurately at a micro level and depict high turnover bone as a low mineralized region, showed that trabecular bones around subchondral cysts consisted of high turnover bone, suggesting subchondral cysts play an important role in the activation of subchondral bone cells. (9) A longitudinal MRI study reported that subchondral cysts appeared in the regions where bone marrow edema had occurred, while other MRI studies indicated a strong relationship between bone marrow edema and cartilage attrition. (10,11) Cyst development and the resulting loss of bone strength sometimes cause a gradual collapse of subchondral bone and progression to joint deformation. Thus, subchondral cysts are deeply related to the progression of OA, and understanding the mechanism of subchondral cyst formation would be meaningful to know more about the pathogenesis of OA.

High-resolution peripheral quantitative computed tomography (HR-pQCT) is a CT scanner that allows one to scan human peripheral skeletal sites such as the distal radius and distal tibia at a high resolution with a voxel size of 82 μm. (12,13) It is also useful for microstructural analysis of comparatively large bone specimens. Bone specimens up to 12.6 cm in diameter and 15 cm in length can be scanned at voxel sizes of 41 μm.

Using HR-pQCT, subchondral cysts can be evaluated three dimensionally and quantitatively at the micro level, which cannot be done with plain radiographs or conventional CT. Moreover, it is possible to evaluate trabecular structure of subchondral bone and areas of cartilage attrition accurately at the same time, allowing analysis of the relationships between subchondral cysts and trabecular bone structure and cartilage attrition.

In this study, femoral heads extracted from hip OA patients were imaged by HR-pQCT, the degree of subchondral cyst formation (volume and number) was investigated, and its correlations with patients' physical and radiological findings, the area of cartilage attrition, and the trabecular structure of subchondral bone were analyzed in order to identify the characteristics of and contributing factors to subchondral cyst formation.

Methods

Materials

Ten patients with dysplastic hip OA who had undergone hip replacement at Nagasaki University Hospital and Nagasaski Yurino Hospital participated in this study (mean age 73±9 years, range 57-83 years, all females). Patients with bone and joint diseases (excluding osteoarthritis) such as osteonecrosis or patients who took medications affecting bone metabolism such as bisphosphonates were excluded from the study. The patients' mean height was 155±6 cm (143-161 cm), weight was 53±10 kg (40-69 kg), body mass index (BMI) was 22±4 kg/m^2 (16-28 kg/m^2), center-edge (CE) angle on the anteroposterior radiographs of the hip joints was 12±10 (-5-26) degrees, and the acetabular angle was 45±5 (40-53) degrees. The CE angle is formed by a line from the center of the femoral head to the lateral edge of the acetabular roof and a vertical line drawn through the center of the femoral head. A low CE angle (<20°) means hip subluxation. The acetabular angle is formed by a horizontal line connecting both tear drops and a line from a tear drop to the lateral edge of the acetabular roof. A high acetabular angle (>45°) means acetabular dysplasia.

Ten femoral head specimens were obtained during surgery and stored in a freezer. The study protocol was approved by the ethics review board of our institute and complied with the Declaration of Helsinki of 1975, revised in 2000.

Imaging

Bone specimens were thawed gradually, put on the dedicated device with the posterior site of the femoral head facing the CT gantry table, and fastened with Velcro. They were scanned using an HR-pQCT (XtremeCT, Scanco Medical, Brüttisellen, Switzerland) with the following scan settings: X-ray tube voltage, 60 kVp; tube current, 900 μAs; exposure time, 300 ms; projection number, 1000; and voxel size, 41 μm. Scan length was approximately 49 mm, resulting in 1200 slices and a 45-minute scan time.

Image Analysis

(1) Cartilage loss area, (2) volume and number of subchondral cysts, and (3) trabecular microstructure in the subchondral bone were measured using bone microstructure measurement software (TRI/3D-BON, Ratoc System Engineering, Tokyo, Japan).

(1) Cartilage loss area—By binarizing CT images using the bone threshold, cortical and cancellous bone were depicted. The threshold value for the binarization was determined by discriminant analysis of the boundary between the bone and background on the histogram of the cancellous bone region. The mean value of 5 arbitrary specimens was used as a fixed threshold value for all specimens. Then, by filling the bone marrow and cyst spaces, a femoral head region was obtained. Subsequently, the outline (1-mm-thick) of the femoral head region was extracted (Fig.1-A).

Next, by binarizing CT images using the soft tissue threshold, both the soft tissue and bone regions were depicted. The threshold value of this binarization was also determined by discriminant analysis in the region, which contains cartilage and air, in the same way as the

bone threshold. Then, by subtracting the femoral head region from these soft tissue and bone regions, only the soft tissue region (cartilage and synovium) was obtained (Fig.1-B). The femoral head outline uncovered by this soft tissue was defined as the cartilage loss region, and its surface area was measured (Fig.1-C, Fig.2-B).

(2) Cyst volume and number—In this study, the region 5 mm below a cartilage loss region was defined as a subchondral bone region (Fig.1-D). A subchondral cyst was defined as a space ≥1 mm in diameter and connecting with the cartilage loss regions. First, by subtracting trabecular bones from the subchondral bone region, both bone marrow and cyst spaces were obtained (Fig.1-E). Then, by eroding these bone marrow and cyst spaces by 0.5 mm from the surface three-dimensionally, spaces <1 mm in diameter were removed (Fig.1-F). The remaining spaces were dilated by 0.5 mm from the surface in order to restore their original shape. Then, by extracting only spaces connected to cartilage loss regions, the subchondral cysts were obtained (Fig.1-G, Fig.2-A). The definition and the extraction method of subchondral cysts were based on our previous study involving high-resolution micro CT. (9)

The following parameters pertaining to the cyst volume and number were measured: total volume of all cysts in the subchondral bone region (Cyst.V) (mm^3), volume percent of all cysts in the subchondral bone region (Cyst.V/TV, cyst volume fraction) (%), total number of all cysts in the subchondral bone region (Cyst.N), number of cysts per unit volume (Cyst.N/TV) ($/cm^3$), average volume of a cyst (CystV.Ave) (mm^3), standard deviation of a cyst volume (CystV.SD) (mm^3), minimum volume of a cyst (CystV.Min) (mm^3), and maximum volume of a cyst (CystV.Max) (mm^3) (Fig.2-A, B).

(3) Trabecular microstructure—Trabecular microstructure was measured in the subchondral bone region excluding the cyst regions (Fig.1-H, I, Fig.2-D). The microstructural parameters measured were: bone volume fraction (BV/TV) (%), trabecular thickness (Tb.Th) (μm), trabecular number (Tb.N) (1/mm), trabecular separation (Tb.Sp) (μm), connectivity density (ConnD) ($1/mm^3$), structure model index (SMI), and degree of anisotropy (DA). (14) ConnD is a parameter of trabecular connectivity, evaluated by Betti number (Conn.D=b1/TV), where a higher value indicates greater connectivity. (15) SMI is an index evaluating whether trabecular bone is rod-like or plate-like, with 0 indicating a plate-like structure and 3 indicating a rod-like structure. (16) DA is evaluated by the ratio between the primary and tertiary axes of the mean intercept length (MIL) ellipsoid (DA=a/c), with a higher value indicating higher anisotropy. (17)

Statistical analysis

Statistical analysis was performed using SPSS ver.16.0 (SPSS, Chicago, IL, USA). The correlations between the cyst parameters and age, height, weight, BMI, the CE angle, the acetabular angle, cartilage loss area, and trabecular microstructural parameters were analyzed using Pearson's correlation coefficient. For all analyses, the level of significance was established at $P < 0.01$.

Results

Tables 1 and 2 show the data on subchondral cyst parameters, cartilage loss area, and trabecular microstructure. As shown in Table 1, Cyst.V/TV was 15%±10% (2-33%), indicating that subchondral cyst formation has a wide range; almost no cysts occurred in one case, while cysts occupied about 30% of subchondral bone in another case. Cyst.N was 26±24 (6-87), and Cyst.N/TV was 4.3±1.9/cm^3 (1.0-6.9). CystV.Ave was 36.9 mm^3, CystV.Min was 1.0 mm^3, and CystV.Max was 657 mm^3. All of these also indicate a wide distribution in number and volume, ranging from a few to multiple, as well as from small to large cyst formation.

As shown in Table 2, the patients had various degrees of cartilage loss areas, ranging from 4.8 to 29.5 cm^2. The average BV/TV was 51.9%, and Tb.Th was 476 μm with the increased bone volume and thickened trabecular bone, which represented bone sclerosis. Average ConnD was 2.14/mm^3, SMI was 0.59, and DA was 1.19, which meant high connectivity, a plate-like structure, and a low degree of anisotropy, respectively.

Table 3 shows the correlations between the cyst parameters and age, physical findings (height, weight, and BMI), radiographic parameters (CE angle, acetabular angle), cartilage loss area, and trabecular microstructural parameters. There were no significant correlations between the cyst parameters and age, physical findings, and radiographic parameters. There was a significant positive correlation between the cartilage loss area and Cyst.N ($r=0.85$, $p<0.01$), indicating that the cases with a large cartilage loss area had a large number of cysts. However, this would not be a significant finding, as there was no significant correlation between the cartilage loss area and Cyst.N/TV, meaning the increased cartilage loss area led to the increased volume of subchondral bone region, which simply resulted in the increased Cyst.N.

There was a significant positive correlation between Cyst.V and BV/TV ($r=0.79$, $p<0.01$), suggesting that cases with a large total volume of cysts had a high bone volume fraction. There were also significant positive correlations between Cyst.N and Tb.Th, and between Cyst.N/TV and BV/TV ($r=0.86$, and $r=0.82$ respectively, both $p<0.01$), meaning cases with multiple cysts had a high bone volume fraction and thickened trabeculae. On the other hand, there were no significant correlations between CystV.Ave and BV/TV or Tb.Th, which means that bone sclerosis was not associated with large cyst formation but multiple cyst formation.

Discussion

In this exploratory study, a three-dimensional micro-structural analysis of subchondral cysts of hip OA patients was conducted using HR-pQCT, and their relationships with cartilage attrition and subchondral bone microstructure were investigated.

The results showed large dispersion in cyst volume fraction, number of cysts, size of each cyst, and structural parameters of trabecular bone (Tables 1 and 2, Fig. 3). These results indicate that bone changes such as subchondral cyst formation and bone sclerosis do not occur in all OA patients homogeneously, but they have various phenotypes.

The patients with a large number of subchondral cysts showed high BV/TV and Tb.Th, indicating that multiple cyst formation is related to bone sclerosis (Table 3). This suggests three possibilities: (1) multiple cyst formation causes bone sclerosis; (2) bone sclerosis leads to multiple cyst formation; and (3) another common factor results in both of them. Specifically, each cyst might cause reactive bone formation around itself, and multiple such areas of reactive bone formation result in bone sclerosis (Fig. 4). (7,8) Alternately, cyst formation might change the mechanical load distribution in subchondral bone, leading to more mechanical stress on the remaining trabecular bones and subsequent bone sclerosis. (18) On the other hand**,** bone sclerosis might prevent large cyst formation, and as a result, a large number of small cysts develops.

The mechanism of subchondral cyst formation in OA is still unknown, but there are mainly two hypotheses. The “synovial fluid intrusion theory” states that a calcified tissue barrier between the cartilage and subchondral bone is broken by the cartilage injuries, and joint fluid intrudes into the bone marrow spaces of the subchondral bone and forms a cyst. (4,6) The “bone contusion theory” states that excessive mechanical stress damages trabecular bones, and the area is absorbed and replaced by a cyst. (5,6) In recent studies, Crema et al. reported a longitudinal MRI study that showed that bone marrow edema lesions in the subchondral bone eventually changed into a cyst. (10) Durr et al. performed finite element analysis and suggested that a subchondral cyst was formed by stress concentration and the subsequent bone resorption. (19) These reports support the “bone contusion theory.” Based on the present study, it is not possible to decide which is the more responsible factor, joint fluid intrusion or bone contusion.

Clinically, these various bone reactions in OA are important to know patients’ natural courses or treatment responses. The biological types of hip OA have been semi-quantitatively classified into hypertrophic, normotrophic, and atrophic types based on degrees of femoral head size and osteophyte formation on plain radiographs. (20) The hypertrophic type is considered to have a comparatively better clinical course, less need for surgical treatments, and better results when osteotomy or joint replacement are performed. (21) On the other hand, the atrophic type tends to have rapid progression, less effect from osteotomy, and more loosening after joint replacement. (22-24) A subchondral cyst could lead to collapse and atrophy of the femoral head; thus, it is considered a poor prognostic factor. Therefore, it is clinically meaningful to evaluate the various bone structure changes including subchondral cysts in patients with hip OA.

HR-pQCT can analyze the bone microstructure of a living human body, but its usage is limited only to peripheral sites, and it is impossible to evaluate hip and knee OA patients at the moment. However, the resolution of clinical CT has developed remarkably in recent years, and quantitative evaluation of trabecular structural changes and small cysts is gradually becoming possible. (25) The resolution of clinical MRI has also improved due to increased magnetic field strength and development of sequences, allowing analysis of small changes in the cartilage and subchondral bone. (26) The results of the present study are expected to provide an important foundation for future studies using these clinical imaging devices. If various bone changes in OA are closely associated with patients’ symptoms and prognosis or their responses to drug therapy and surgery, subchondral bone structural

analysis will become a useful evaluation factor in clinical practice. Moreover, if we can unravel the mechanism of subchondral cyst formation and develop a method to prevent cyst formation, it would become a new treatment for OA.

This study has several limitations. First, the number of cases was small, and no definite conclusions are possible; this was an exploratory study. In order to identify only obvious findings, the significance level was set at $P<0.01$. Second, this was a cross-sectional study using only advanced dysplastic hip OA cases with no controls. There was also no histological or biochemical analysis. Thus, no conclusion about the pathogenesis of OA initiation or primary hip OA can be made. Further longitudinal studies using clinical CT could be one way to obtain a better understanding. Comparison of HR-pQCT images with histology, clinical symptoms, or MR images would also provide more useful information.

One of the definitions of a subchondral cyst in this study was a space >1 mm in diameter, so subchondral cysts <1 mm in diameter were not evaluated. When we extracted spaces <1 mm in diameter, a huge number of normal bone marrow spaces was obtained. It is impossible to differentiate tiny subchondral cysts from normal bone marrow. The other definition of a subchondral cyst was a space connected with a cartilage loss region. Subchondral bone occasionally contains wide normal bone marrow spaces >1 mm in diameter in the deep layer. They could be deleted by extracting only spaces connected with the cartilage loss region. These definitions were set and confirmed by our previous study using high-resolution micro CT. (9) Regarding the volume of subchondral cysts, it was impossible to differentiate multiple cysts connecting to each other from a large solitary cyst with a large diameter, and these were thus regarded as similar large cysts, although they were formed in a different way. Likewise, it was inevitable that the total number of subchondral cysts decreased when multiple cysts were connected to each other.

In conclusion, a quantitative evaluation method to measure the degree of subchondral cyst formation of hip OA was proposed. The cyst volume fraction in subchondral bone, their number, and their individual sizes varied widely depending on the patients, suggesting that bone changes due to OA had various types according to patients' specific biological reactions. There was a strong relationship between multiple cyst formation and bone sclerosis, which might have been caused by reactive bone formation that occurred around each cyst. Since bone structural changes in OA are related to clinical results, the quantitative analysis of subchondral cysts could become a useful evaluation item for the future clinical assessment of OA.

Acknowledgments

The authors would like to thank Ryoichi Takasuga (Department of Orthopedic Surgery, Nagasaki Yurino Hospital, Nagasaki, Japan) for collecting the bone specimens. This research was supported by NIH R01 AG17762 (SM).

References

1. Lories RJ, Luyten FP. The bone–cartilage unit in osteoarthritis. Nat Rev Rheumatol. Jan 7; 2011 7(1):43–9. [PubMed: 21135881]

2. Hayami T, Pickarski M, Zhuo Y, Wesolowski GA, Rodan GA, Duong LT. Characterization of articular cartilage and subchondral bone changes in the rat anterior cruciate ligament transection and meniscectomized models of osteoarthritis. Bone. Feb 1; 2006 38(2):234–43. [PubMed: 16185945]
3. Hayami T, Pickarski M, Wesolowski GA, Mclane J, Bone A, Destefano J, et al. The role of subchondral bone remodeling in osteoarthritis: Reduction of cartilage degeneration and prevention of osteophyte formation by alendronate in the rat anterior cruciate ligament transection model. Arthritis Rheum. Apr 1; 2004 50(4):1193–206. [PubMed: 15077302]
4. Freund E. The pathological significance of intra-articular pressure. Edinburgh Med J. 1940; 47:192.
5. RHANEY K, LAMB DW. The cysts of osteoarthritis of the hip; a radiological and pathological study. J Bone Joint Surg Br. Nov 1; 1955 37-B(4):663–75. [PubMed: 13271499]
6. Resnick D, Niwayama G, Coutts RD. Subchondral cysts (geodes) in arthritic disorders: pathologic and radiographic appearance of the hip joint. AJR Am J Roentgenol. May 1; 1977 128(5):799–806. [PubMed: 404905]
7. Havdrup T, Hulth A, Telhag H. The subchondral bone in osteoarthritis and rheumatoid arthritis of the knee. A histological and microradiographical study. Acta Orthop Scand. Jun 1; 1976 47(3):345–50. [PubMed: 952224]
8. Sabokbar A, Crawford R, Murray DW, Athanasou NA. Macrophage-osteoclast differentiation and bone resorption in osteoarthrotic subchondral acetabular cysts. Acta Orthop Scand. Jun 1; 2000 71(3):255–61. [PubMed: 10919296]
9. Chiba K, Nango N, Kubota S, Okazaki N, Taguchi K, Osaki M, et al. Relationship between microstructure and degree of mineralization in subchondral bone of osteoarthritis: A synchrotron radiation μCT study. J Bone Miner Res. Jun 15; 2012 27(7):1511–7. [PubMed: 22434696]
10. Crema MD, Roemer FW, Zhu Y, Marra MD, Niu J, Zhang Y, et al. Subchondral cystlike lesions develop longitudinally in areas of bone marrow edema-like lesions in patients with or at risk for knee osteoarthritis: detection with MR imaging--the MOST study. Radiology. Sep 1; 2010 256(3): 855–62. [PubMed: 20530753]
11. Taljanovic MS, Graham AR, Benjamin JB, Gmitro AF, Krupinski EA, Schwartz SA, et al. Bone marrow edema pattern in advanced hip osteoarthritis: quantitative assessment with magnetic resonance imaging and correlation with clinical examination, radiographic findings, and histopathology. Skeletal Radiol. Feb 15; 2008 37(5):423–31. [PubMed: 18274742]
12. Burghardt AJ, Link TM, Majumdar S. High-resolution Computed Tomography for Clinical Imaging of Bone Microarchitecture. Clin Orthop Relat Res. Aug 23; 2011 469(8):2179–93. [PubMed: 21344275]
13. Patsch JM, Burghardt AJ, Kazakia G, Majumdar S. Noninvasive imaging of bone microarchitecture. Annals of the New York Academy of Sciences. Dec 1.2011 1240:77–87. [PubMed: 22172043]
14. Hildebrand T, Rüegsegger P. A new method for the model-independent assessment of thickness in three-dimensional images. J Microsc. Jan 9; 1997 185(1):67–75.
15. Odgaard A, Gundersen HJ. Quantification of connectivity in cancellous bone, with special emphasis on 3-D reconstructions. Bone. 1993; 14(2):173–82. [PubMed: 8334036]
16. Hildebrand T, Rüegsegger P. Quantification of Bone Microarchitecture with the Structure Model Index. Comput Methods Biomech Biomed Engin. 1997; 1(1):15–23. [PubMed: 11264794]
17. Whitehouse WJ. The quantitative morphology of anisotropic trabecular bone. J Microsc. Jul 1; 1974 101(Pt 2):153–68. [PubMed: 4610138]
18. Mcerlain DD, Milner JS, Ivanov TG, Jencikova-Celerin L, Pollmann SI, Holdsworth DW. Subchondral cysts create increased intra-osseous stress in early knee OA: A finite element analysis using simulated lesions. Bone. Mar 1; 2011 48(3):639–46. [PubMed: 21094285]
19. Dürr HD, Martin H, Pellengahr C, Schlemmer M, Maier M, Jansson V. The cause of subchondral bone cysts in osteoarthrosis: a finite element analysis. Acta Orthop Scand. Oct 1; 2004 75(5):554–8. [PubMed: 15513486]
20. Bombelli, R. Osteoarthritis of the Hip: Classification and Pathogenesis: The Role of Osteotomy as a Consequent Therapy. Springer; Berlin Heidelberg New York: Feb 27. 1983 p. 98-108.
21. Solomon L, Schnitzler CM. Pathogenetic types of coxarthrosis and implications for treatment. Arch Orthop Trauma Surg. 1983; 101(4):259–61. [PubMed: 6882165]

22. Saito M, Saito S, Ohzono K, Ono K. The osteoblastic response to osteoarthritis of the hip. Its influence on the long-term results of arthroplasty. J Bone Joint Surg Br. Nov; 1987 69(5):746–51. [PubMed: 3680335]

23. Hernández-Vaquero D, Suárez-Vazquez A, Fernández-Corona C, Menéndez-Viñuela G, Alegre-Mateo R, García-Sandoval MA. Loosening of threaded acetabular cups in arthroplasty of the hip. The association with different types of coxarthrosis. International Orthopaedics (SICOT). 1996; 20(2):70–4.

24. Kobayashi S, Takaoka K, Saito N, Hisa K. Factors affecting aseptic failure of fixation after primary Charnley total hip arthroplasty. Multivariate survival analysis. J Bone Joint Surg Am. Nov; 1997 79(11):1618–27. [PubMed: 9384420]

25. Chiba K, Ito M, Osaki M, Uetani M, Shindo H. In vivo structural analysis of subchondral trabecular bone in osteoarthritis of the hip using multi-detector row CT. Osteoarthr Cartil. Feb 1; 2011 19(2):180–5. [PubMed: 21087677]

26. Krug R, Banerjee S, Han ET, Newitt DC, Link TM, Majumdar S. Feasibility of in vivo structural analysis of high-resolution magnetic resonance images of the proximal femur. Osteoporos Int. Nov 6; 2005 16(11):1307–14. [PubMed: 15999292]

Highlight

- A three-dimensional analysis of subchondral cysts was conducted using HR-pQCT.
- The degree of cyst formation showed a wide distribution in number and volume.
- There was a close relationship between multiple cyst formation and bone sclerosis.

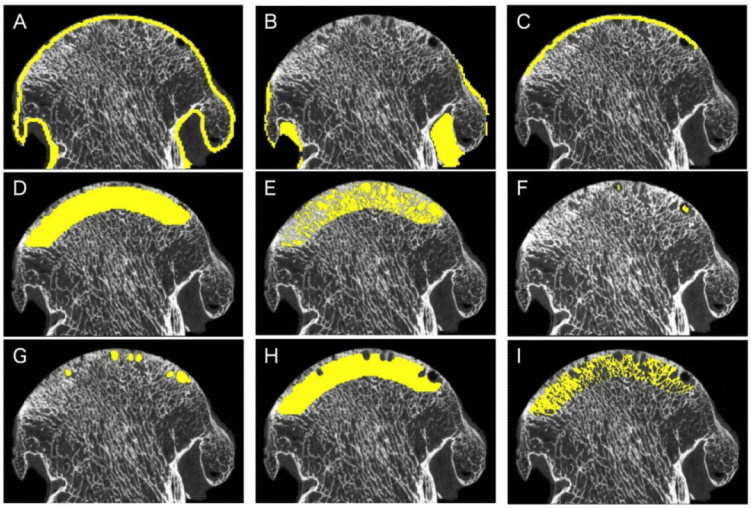

Fig. 1.

(A-C): A cartilage loss region is defined as the femoral head outline uncovered by soft tissues, and its surface area is measured. (D): A subchondral bone region is defined as a region 5 mm under the cartilage loss region. (E-G): Subchondral cysts are defined as spaces >1 mm in diameter and connected with the cartilage loss regions, and their volume and number are measured. By eroding bone marrow and cyst spaces 0.5 mm from their surfaces, spaces <1 mm in diameter vanish. In this step, most of the normal bone marrow spaces could be deleted. By dilating the remaining spaces 0.5 mm from their surfaces and extracting only the spaces connected to cartilage loss regions, subchondral cysts could be obtained. (H-I): Subchondral trabecular structure is measured in the subchondral bone region, excluding cyst regions.

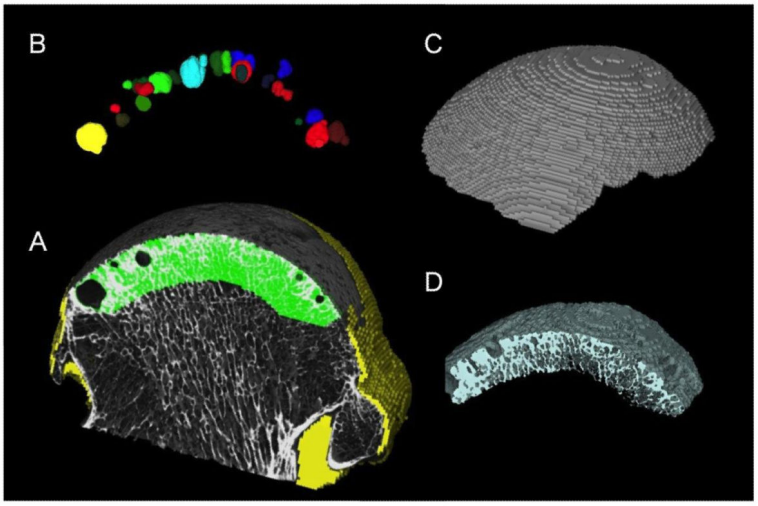

Fig. 2.

3D CT images of (A) femoral head with OA, (B) subchondral cysts, (C) cartilage loss region, and (D) subchondral trabecular bone. The subchondral bone region is shown as green and soft tissue as yellow. The different colors of subchondral cysts mean that there is no connectivity between them.

The following cyst related parameters are measured: Cyst.V: Total volume of all cysts in the subchondral bone region. Cyst.V/TV: Cyst volume fraction. Cyst.N: Total number of cysts in the subchondral bone region. Cyst.N/TV: Number of cysts per unit volume. CystV.Ave: Average volume of each cyst. CystV.SD, CystV.Min, CystV.Max: SD, minimum, and maximum volume of each cyst.

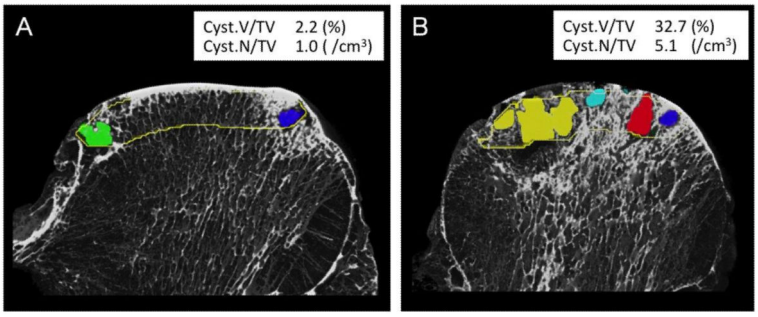

Fig. 3.

Distribution of subchondral cysts in the subchondral bone region (yellow line).

The volume and number of cysts are extremely different among individuals. Cyst volume fraction (Cyst.V/TV) ranges from 2.2% to 32.7%.

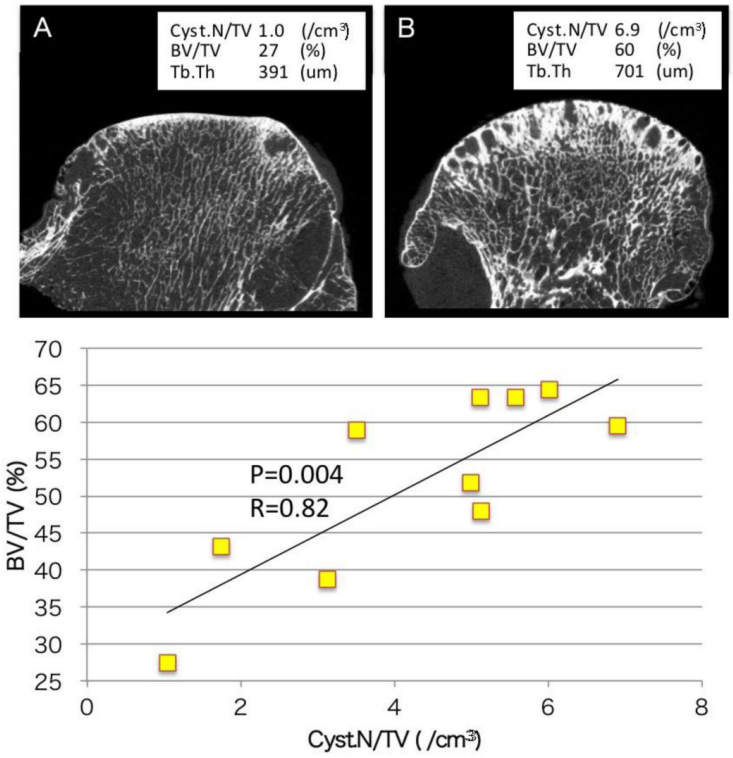

Fig. 4.

Cyst.N/TV and BV/TV have a positive correlation (P<0.004, R=0.82), suggesting that multiple cyst formation is related to bone sclerosis.

(A-B): 2D images of OA femoral heads show that the trabecular bone sclerosis occurs particularly around the cysts. These areas of bone sclerosis might be caused by the reactive bone formation against bone absorption or the change of mechanical load distribution in the subchondral bone.

Table. 1

Cyst parameters

	CystV (mm^3)	Cyst.V/TV (%)	Cyst.N	Cyst.NI/TV ($/cm^3$)	CystV.Ave (mm^3)	CystV.SD (mm^3)	CystV.Min (mm^3)	CystV.Max (mm^3)
Ave	718	14.5	26	4.3	36.9	85.8	1.2	331
SD	432	9.6	24	1.9	26.3	64.3	0.3	236
Min	172	2.2	6	1.0	8.3	8.6	1.0	37
Max	1363	32.7	87	6.9	91.3	195.1	2.0	657

Table.2

Cartilage loss area and bone microstructural parameters

	Cart. Loss (cm^2)	BV/TV (%)	Tb.Th (μm)	Tb.N (/mm)	Tb.Sp (μm)	Conn.D ($/mm^3$)	SMI	DA
Ave	13.7	51.9	476	0.575	426	2.14	0.59	1.19
SD	7.0	12.4	99	0.115	93	0.62	0.94	0.12
Min	4.8	27.4	387	0.361	299	1.09	−0.54	1.09
Max	29.5	64.4	701	0.743	626	3.16	2.45	1.40

Table.3

Correlation coefficients between cyst parameters and physical findings, cartilage loss area, and bone microstructural parameters

	Cyst.V	Cyst.V/TV	CystN	Cyst.N/TV	CystVAve	CystV.SD	CystV.Min	CystV.Max
Age	−0.01	−0.22	0.06	−0.44	0.17	0.04	0.38	−0.14
Height	−0.47	−0.52	0.03	−0.13	−0.43	−0.57	0.30	−0.58
Weight	0.20	0.49	−0.10	0.34	0.36	0.33	−0.42	0.32
BMI	0.35	0.66	−0.12	0.37	0.50	0.52	−0.49	0.51
CE angle	−0.44	−0.29	−0.44	−0.77	0.34	0.22	0.29	−0.12
Acet. angle	0.32	0.25	0.58	0.70	−0.13	−0.22	−0.38	−0.21
Cart.Loss	0.22	−0.40	0.85*	0.38	−0.62	−0.58	0.10	−0.39
BV/TV	0.79*	0.69	0.44	0.82*	0.14	0.21	−0.69	0.40
Tb.Th	0.59	0.04	0.86*	0.71	−0.35	−0.29	−0.44	−0.04
Tb.N	−0.04	0.53	−0.67	−0.23	0.73	0.71	−0.30	0.49
Tb.Sp	−0.53	−0.71	−0.02	−0.55	−0.24	−0.29	0.66	−0.40
Conn.D	−0.75	−0.37	−0.53	−0.58	0.09	−0.03	0.13	−0.35
SMI	−0.68	−0.73	−0.16	−0.64	−0.26	−0.37	0.66	−0.53
DA	−0.52	−0.46	−0.24	−0.61	−0.12	−0.30	0.69	−0.49

* Pearson's correlation coefficient P<0.01